ACS Sustainable Chemistry & Engineering

pubs.acs.org/journal/ascecg

Research Article

Aqueous and Biphasic Coupling of Furfural and Cyclopentanone for the Synthesis of Bio-Jet Fuel Precursors

Rick Baldenhofer, Jean-Paul Lange, Sascha R. A. Kersten, and M. Pilar Ruiz*

Cite This: https://doi.org/10.1021/acssuschemeng.4c09269

Read Online

ACCESS | Metrics & More | Article Recommendations | Supporting Information

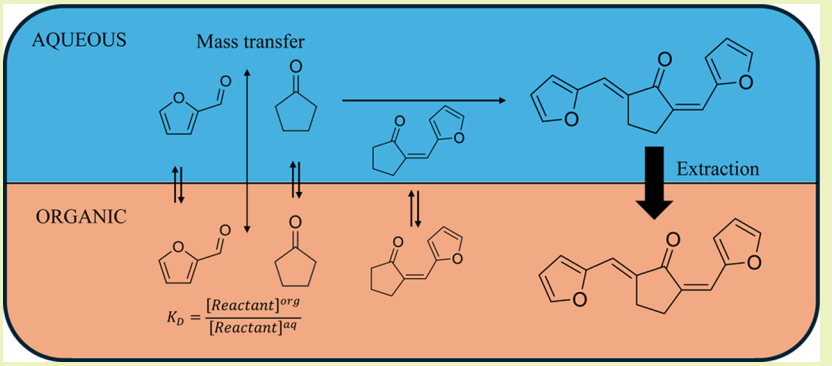

ABSTRACT: We report on the aldol condensation of furfural and cyclopentanone in aqueous and biphasic mediums as a promising step for producing sustainable aviation fuel. Key parameters, including catalyst concentration, reactant concentration, temperature, and solvent, were found to significantly influence conversion and product selectivity. Alkaline conditions were essential for aldol coupling, with significant conversion observed at pH 12 and higher. The activation energies for the formation of the dimeric and trimeric aldol adducts were similar at 74 and 76 kJ/mol, respectively. Biphasic conditions were employed to prevent product precipitation, leading to reactor and equipment fouling. For biphasic conditions, the extraction of the reactants and dimeric intermediates to the organic phase affected rate and selectivity, resulting in the dilemma. Good product extraction leads to inevitable reactant extraction. Based on these findings, an integrated biphasic process design was proposed, utilizing process-owned solvents to optimize the separation and recycling of aqueous streams and improve the overall process efficiency.

KEYWORDS: *aldol condensation, sustainable aviation fuel, biphasic system, reactive extraction, furfural*

1. INTRODUCTION

The aviation industry has long relied on fossil-based jet fuels, contributing significantly to global carbon emissions and environmental degradation. As concerns over climate change and energy sustainability intensify, the transition from fossil fuels to renewable alternatives has become imperative.[1−4]

While sectors such as building, light duty road transportation, and light industries have experienced significant advancements in electrification, long-haul heavy-duty transport has largely resisted this shift. The primary challenge of this sector lies in the low energy density of current battery technologies, which renders them insufficient for the high energy demands of heavy-duty applications. Consequently, this sector remains reliant on hydrocarbon fuels for the foreseeable future.[5,6]

Recent advances have been made in the synthesis of renewable transportation fuels. Jet fuel can be derived from a variety of biobased feedstocks such as waste cooking/vegetable oils (HEFA-process),[7,8] the conversion of captured CO_2 to methanol (methanol-to-jet),[9−12] sugar fermentation to alcohols,[13−15] (alcohol-to-jet), gasification of biomass to syngas utilizing the Fischer−Tropsch process,[9] and a variety of lignocellulosic biomass-derived routes.[16−21]

The latter is of particular interest as it is one of the planet's most abundant resources of renewable carbon. Notably, furfural (FUR), synthesized from lignocellulosic biomass, has garnered significant attention for its versatile applications in renewable chemical and fuel production.[18,22−28]

Extracted from agricultural residues such as corn cobs, oat hulls, bagasse, and wood chips, FUR serves as a crucial intermediate in the synthesis of various high-value products, including solvents, resins, and specialty chemicals.[22,23,25,29] But FUR has also emerged as a sustainable source of jet and diesel fuel precursors, attracting significant attention from researchers

Received: November 7, 2024
Revised: December 10, 2024
Accepted: December 12, 2024

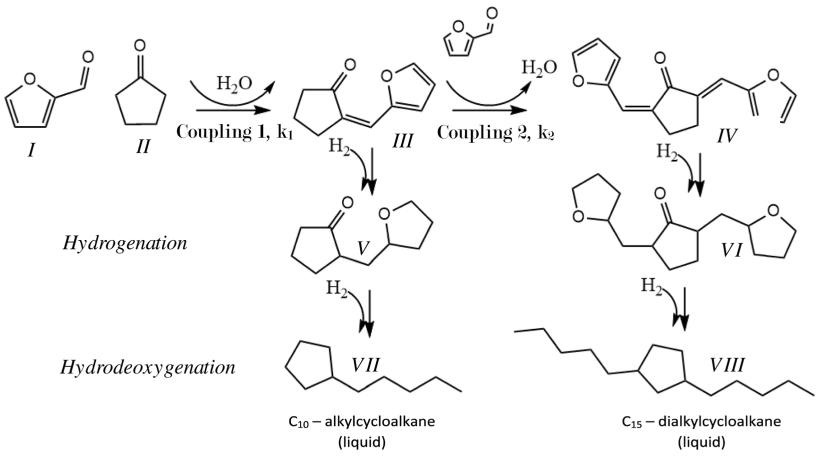

Figure 1. Route for upgrading FUR to jet and diesel range fuel via the aldol condensation of FUR with CPO.

and the aviation industry alike. The literature documents several pathways for upgrading FUR toward jet- and diesel-range hydrocarbons, all involving C−C coupling followed by deep hydrogenation.

One particularly intriguing route involves the aqueous phase aldol condensation of FUR with cyclopentanone (CPO), a cyclic ketone that can be derived from FUR itself (Figure 1).[30−33] This coupling delivers dimeric C10 (III) and trimeric C15 (IV) precursors, which can be effectively upgraded to (di)alkyl cycloalkanes (VII and VIII), known for their desirable fuel properties.[34]

Unfortunately, this route is not without its challenges. While the aqueous phase aldol condensation already performs well under mild operating conditions (e.g., room temperature and atmospheric pressure), processes encounter operational challenges such as equipment corrosion. Additionally, C10 and C15 aldol adducts are notoriously insoluble in a range of common solvents including water. This insolubility leads to product deposition and clogging, necessitating dedicated engineering and specialized reactor design. To partly address these issues, researchers have transitioned from aqueous to organic conditions but still encounter operational challenges, especially with product and solvent separation and the generation of "heavy" side products.[35]

Biphasic dehydration could alleviate some of these challenges. This approach makes use of an aqueous reactive phase and an organic extractive phase, reactive extraction. It will allow for increased product solubility and easy separation through phase separation while decreasing the aqueous phase holdup, which is advantageous for corrosion prevention.

While the use of cosolvents or biphasic conditions is not new,[36] their implementation has predominantly relied on "process-foreign" solvents (e.g., solvents that are not present in the process) and heterogeneous catalysts, leading to significantly extended reaction times and necessitating (complex) downstream solvent separation. Additionally, the combined influence of reaction parameters and their impact on reaction kinetics in the presence of a biphasic system have not been thoroughly explored.

This paper aims to overcome the limitations of aqueous operations by shifting to a biphasic medium and exploring process-owned cosolvents. Before biphasic systems could be explored, the first parameters influencing the monophasic aqueous aldol condensation were determined, such as temperature, feed concentration, and catalyst concentration (pH). The experimental data were used to develop a simple first-order kinetic model. Subsequently, biphasic studies were conducted. Various solvents were evaluated, and the resulting data are analyzed using LLE data and a slightly modified kinetic model developed for biphasic conditions. This ultimately leads to a proposed conceptual process design.

2. MATERIALS AND METHODS

2.1. Materials. FUR (≥99%), furfuryl alcohol (≥98%), cyclopentanol (99%), CPO (99%), hydrochloric acid, phosphoric acid, sodium hydroxide (pellets), ethyl acetate (99.5%), decahydronaphthalene (decalin), guaiacol, 2-methyl-tetrahydrofuran (THF), octane, heptane, DMSO, and ethanol were purchased from Sigma-Aldrich. Pentadecane was purchased from BLDpharm.

2.2. Aqueous and Biphasic Experiments. The aqueous aldol condensation experiments were conducted in a 250 mL glass-jacketed reactor operated under atmospheric pressure. The glass jacketed reactor was heated by attaching a temperature-controlled water bath, with monitoring of the water and reactor temperature. The liquid phase was stirred by a mechanical stirrer that was powered by a 0−15 V power supply.

Typically, certain amounts of FUR and CPO were added to the reactor at a stoichiometric molar ratio of 2:1 (unless specified otherwise), together with 100 mL of demineralized water that was conditioned at the desired pH by the addition of NaOH or H_3PO_4. As the reaction proceeded at room temperature under alkaline conditions, samples were taken and acidified to stop the reaction. Afterward the reaction mixture was filtered over a Büchner funnel under suction, and the filter cake was washed twice with 0.5 L of deionized water and dried overnight at 105 °C.

In biphasic experiments, water was exchanged partly by the addition of organics. The volumetric ratio of organic to water was changed as desired. Importantly, the aqueous and organic phases were first saturated in organic solvent and water to maintain the correct volumetric ratios. Experiments were performed following the same procedure as that applied for monophasic aqueous experiments.

2.3. Product Recrystallization for Calibration. Due to limited commercial availability or high costs, the aldol adducts were synthesized in-house for the calibration of analytical equipment. To purify the reaction products, recrystallization was performed on the aldol adducts. Specifically, the trimeric adducts were crystallized from an ethyl acetate solution heated to 70 °C in a beaker on a heating plate. A measured amount of the aldol product was added to the solution, and the mixture was stirred gently for several minutes. The beaker was then removed from the heat source and placed in an ice bath to allow the solution to cool, facilitating the recrystallization. The solution was left undisturbed for 30 min, after which the crystals were collected via vacuum filtration using a Büchner setup.

https://doi.org/10.1021/acssuschemeng.4c09269
ACS Sustainable Chem. Eng. XXXX, XXX, XXX−XXX

2.4. Analysis. Reaction products were analyzed both quantitatively and qualitatively using a GC 7890A MS 5975C by Agilent Technologies with an autosampler and a flame ionization detector (FID). The GC column was an Agilent VF-1701 ms. The column temperature was initially kept at 45 °C for 10 min and then increased at a rate of 3 °C per minute to 280 °C.

Conversion, selectivity, and yield were expressed as mol % of CPO and FUR as defined by eqs I–III resulting in dedicated CPO and FUR balances.

As only the trimeric species were synthesized in-house, the response factors for dimer calibrations used in GCMS were determined theoretically. Using the method described by Laumer et al., FID response factors could be theoretically predicted using the enthalpies of combustion and their corresponding molecular structure. The whole procedure can be found in their publication.[37]

$$\text{Conversion (mol \%)} = \left(1 - \frac{\text{mole CPO end}}{\text{mole CPO start}}\right) \times 100 \quad \text{(I)}$$

$$\text{Selectivity (mol \%)} = \left(\frac{\text{mole of CPO in product}}{\text{mole CPO loaded} - \text{mole CPO end}}\right) \times 100 \quad \text{(II)}$$

$$\text{Yield (mol \%)} = \left(\frac{\text{mole of CPO in products}}{\text{mole CPO loaded}}\right) \times 100 \quad \text{(III)}$$

3. MONOPHASIC SYSTEM: VALIDATION OF PRIOR ART

Our initial focus was on confirming the prior art on aqueous operation. The experimental results were used to develop a simple first-order kinetic model to evaluate the influence of key parameters. Next, biphasic systems were investigated.

3.1. Reaction Mechanism and Kinetic Model. The formation of C10–C15 aldol adducts proceeds through a sequential aldol coupling of FUR and CPO. The carbonyl of CPO is activated through α-hydrogen abstraction leading to an enolate species (Figure 2). Through a nucleophilic attack, this

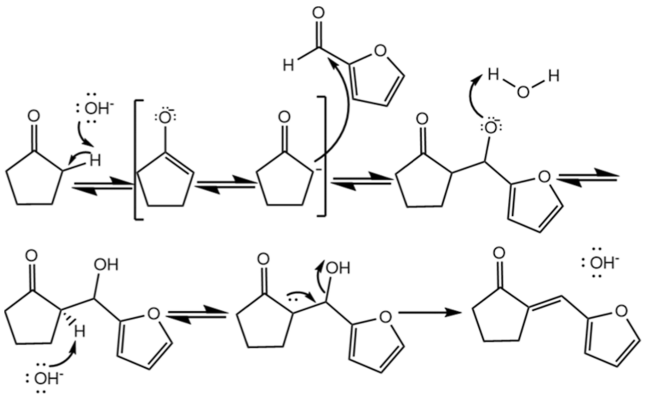

Figure 2. Aldol condensation mechanism for the coupling of CPO and FUR using NaOH.

enolate species attacks the aldehyde, forming a α,β-unsaturated carbonyl compound (C10) after dehydration. As CPO has α-hydrogens at each side of the carbonyl, it can undergo a second coupling according to the same mechanism, forming C15 adducts. The progress of the reaction illustrated in Figure 3 could be modeled by applying a simple first-order kinetic model and solving differential eqs IV–VII.

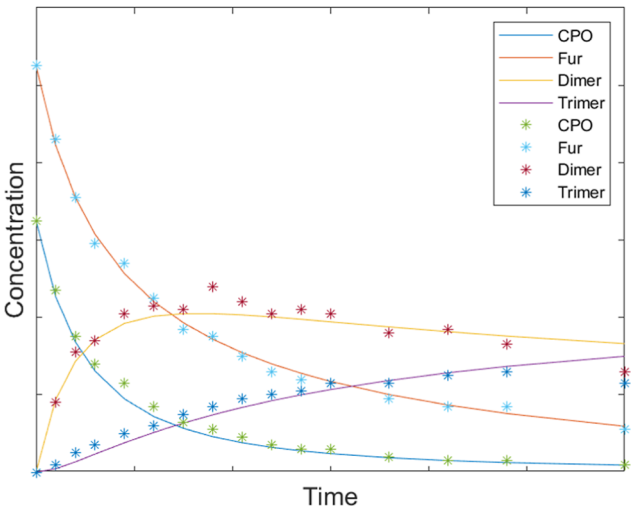

Figure 3. Example of fitting of the experimental data of FUR, CPO, and dimeric and trimeric products using a first-order kinetic model (parity plots: Figure S1).

$$\frac{\text{d[CPO]}}{\text{d}t} = -k_1[\text{CPO}][\text{FUR}] \quad \text{(IV)}$$

$$\frac{\text{d[FUR]}}{\text{d}t} = -k_1[\text{CPO}][\text{FUR}] - k_2[\text{dimer}][\text{FUR}] \quad \text{(V)}$$

$$\frac{\text{d[dimer]}}{\text{d}t} = k_1[\text{CPO}][\text{FUR}] - k_2[\text{dimer}][\text{FUR}] \quad \text{(VI)}$$

$$\frac{\text{d[trimer]}}{\text{dt}} = k_2[\text{dimer}][\text{FUR}] \quad \text{(VII)}$$

3.2. Effect of [OH$^-$]. Although the literature reports a wide operating window for the aldol condensation reaction, we revisited the reaction's activity under both acidic and alkaline conditions. Batch experiments conducted in the acidic regime, with pH ranging from 1 to 7 using H_3PO_4 at room temperature, showed no conversion or product formation across the entire acidic range (results not shown here).

Moving to alkaline conditions using NaOH, a strong increase in activity starting around pH 12.0 was observed. Using our kinetic model, the experimental data were fitted and kinetic constants k_1 and k_2 could be determined, as shown in Figure 4.

A power law relation for both the first (dimeric) and second (trimeric) coupling constants were found according to VIII, as fitted in Figure 4.

$$k_{\text{obs}} = k_0 \times [\text{OH}^-]^a \quad \text{(VIII)}$$

Although the first and second coupling reactions are expected to follow the same mechanism outlined in Figure 2, the observed reaction orders differ, with the first coupling showing a power of approximately $a = 1.5$, while the second exhibits $a = 1.0$.

The relationship between k_1 and k_2 becomes more apparent when product selectivity is examined as a function of [OH$^-$] at a fixed CPO conversion of 50%, shown in Figure 5. The model appears to be in agreement with the experimental results. At lower [OH$^-$] levels, product selectivity shifts toward a higher trimer to dimer ratio at constant conversion, consistent with the data presented in Figure 4. At relatively low [OH$^-$], the difference in rate constant is less pronounced compared to

https://doi.org/10.1021/acssuschemeng.4c09269
ACS Sustainable Chem. Eng. XXXX, XXX, XXX−XXX

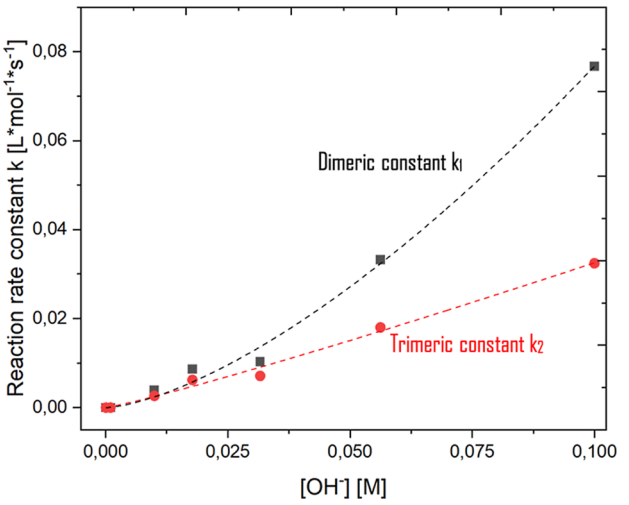

Figure 4. Influence of [OH^-] on the aldol condensation reaction for both the first (k_1) and second (k_2) coupling [CPO and FUR: 2.63 and 6.0 wt % (1:2 mol/mol), 30 °C].

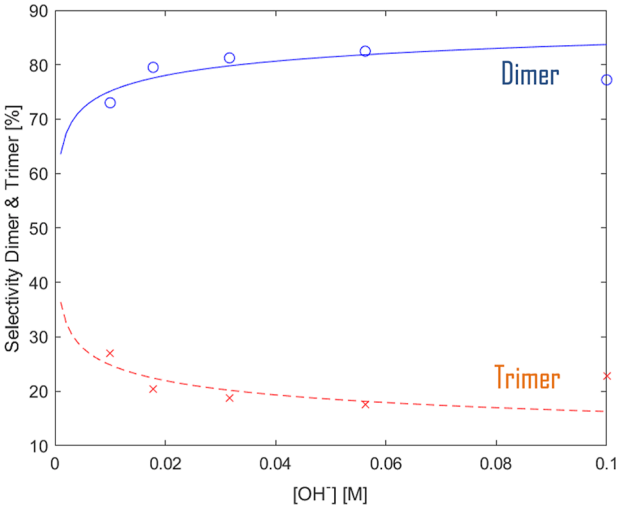

Figure 5. Selectivity of trimeric and dimeric aldol adducts as a function of pH was evaluated at 50% CPO conversion, with experimental data for the dimer (o) and trimer (x) and respective fitting (continuous and dashed lines) [CPO and FUR: 2.63 and 6.0 wt % (1:2 mol/mol, 30 °C)].

higher [OH^-] levels. Similarly at increased [OH^-], at higher levels of conversion, there still appears to be an accumulation of the dimeric aldol adduct, indicating that the gap between k_1 and k_2 increases as a function of [OH^-].

Although the second coupling can be considered identical to the first coupling in terms of the reaction mechanism, a different sensitivity to [OH^-] is observed.

One could expect $k_{2,o} \sim \frac{k_{1,0}}{2}$ by the fact that CPO offers two sides to form the dimer but only one to form the trimer. But this would not explain the difference in reaction order a vs [OH^-]. An alternative explanation could lie in an electronic effect of the enolate species: the negative charge of the enolate species is more delocalized on the dimer than on CPO, which affects both the ease of deprotonation and the nucleophilicity of the intermediate.

In addition, operating at high pH while reducing residence times and maintaining lower FUR conversion increases flexibility in controlling product distribution, favoring the formation of C10 over C15 adducts.

Additionally, the literature indicates that ketones can undergo self-condensation, a reaction where two ketone molecules react with each other rather than with a present aldehyde. Under the performed experimental conditions, no CPO coupled adducts (neither dimeric, trimeric, or tetrameric) were observed. This strongly indicated that the rate of FUR−CPO coupling is much more favored than self-condensation of CPO ($rate_{FUR\text{-}CPO} \gg rate_{CPO\text{-}CPO}$), which is consistent with the higher electrophilicity of aldehydic carbonyls even when bound to an aromatic group.

3.3. Effect of Temperature. Experiments conducted at various temperatures yielded data to construct the Arrhenius plot shown in Figure 6. The first-order kinetic rate constants k_1 and k_2 showed very similar activation energies around 75 kJ/mol, with k_1 being about 4.5× higher than k_2, as illustrated in Figure 6.

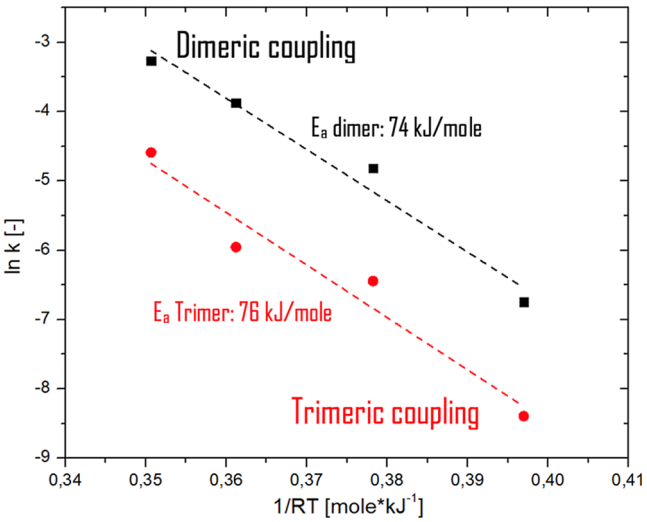

Figure 6. Arrhenius plot plotting kinetic constants k_1 and k_2 for the aldol condensation of FUR and CPO. Temperature range of 30−70 °C, CPO and FUR: 2.63 and 6.0 wt %, at pH 12.

The variation in the reaction temperature did not have a significant impact on selectivity, as demonstrated in Figure 7, which presents both the model and experimental selectivity at a fixed CPO conversion of 50%. This observation is consistent with the similar activation energies observed for both coupling reactions.

3.4. Effect of Excess Reactant. To assess the impact of excess FUR on the reaction rate and product selectivity, experiments were conducted with varying FUR/CPO molar ratios ranging from 2 to 5.5. It is crucial to highlight that all concentrations were carefully selected to maintain monophasic conditions throughout the reactions by keeping the FUR concentration constant while reducing the CPO concentration.

The experimental data showed that increasing the FUR concentration led to a corresponding increase in the CPO conversion rate, with higher stoichiometry resulting in a shorter reaction time to reach 50% CPO conversion (Figure 8). While the time differences to reach 50% conversion may appear minimal in Figure 8, excess FUR has a significant impact on the overall conversion rate when considering near 100% CPO conversion, as illustrated in Figures S2 and S3, and

https://doi.org/10.1021/acssuschemeng.4c09269
ACS Sustainable Chem. Eng. XXXX, XXX, XXX−XXX

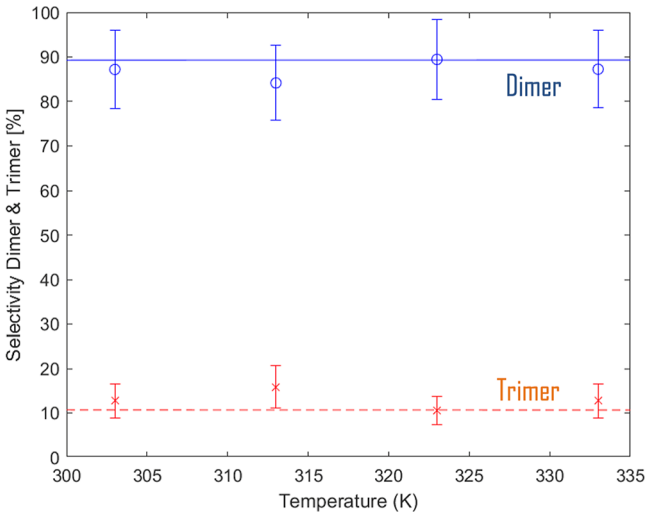

Figure 7. Selectivity of trimeric and dimeric aldol adducts as a function of temperature was evaluated at 50% CPO conversion, with experimental data for the dimer (o) and trimer (x) and respective fitting (continuous and dashed lines), CPO and FUR: 2.63 and 6.0 wt % (1:2 mol/mol).

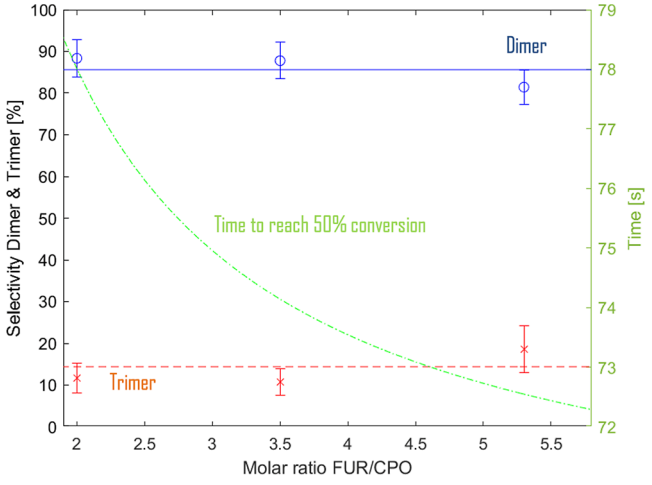

Figure 8. Experimental and modeled product selectivity as a function of the CPO/FUR ratio at a fixed amount of CPO of 2.6 wt %, pH 12.5, 30 °C at 50% CPO conversion.

can therefore be misleading. However, operating with a high excess of reactant may not be ideal for industrial applications due to operational constraints and product and unconverted reactant separation challenges, making such conditions impractical.

In terms of selectivity, no significant enhancement in the trimeric selectivity was observed experimentally, which is consistent with the kinetic model. This is expected as all rate equations exhibit a first-order dependency on the FUR concentration, equally affecting its rate and therefore selectivity at fixed conversion.

3.5. Biphasic Conditions. The aqueous reaction described above presents significant challenges, including product precipitation, which leads to fouling, the generation of alkaline wastewater streams, and material corrosion. Industrially, some of these issues could be overcome by using a biphasic system that extracts the product.

The use of cosolvents in aldol condensation is not a new concept, as it was previously proposed by Cueto et al. in 2017, who explored monophasic cosolvents to enhance product solubility. However, this approach introduces added complexity in the separation process involving the product, caustic water, and the cosolvent. Moreover, the specific impact of utilizing biphasic systems on the reaction performance remains insufficiently understood.

The use of biphasic systems was revisited, utilizing various organic solvents and different water-to-organic volume ratios to investigate their effects on reaction kinetics with the aim of preventing fouling. Since organic solvents appeared to influence not only product solubility but also reaction kinetics, a more comprehensive understanding of their role under biphasic conditions was sought through the use of an extended kinetic model.

3.6. Effect of Solvent. Various organic solvents were explored for their use in a biphasic system, including 2-MTHF, a product of selective FUR hydrogenation, guaiacol, decalin, and octane. These solvents exhibit different reactant partition coefficients (K_d) for CPO and FUR, which were found to vary from 0.6 to 3.2 for CPO and 0.4 to 5.1 for FUR. Using these solvents, experiments were performed at different volumetric ratios of water and organic.

Utilizing 2-MTHF ($K_{d,CPO}$ = 3.2, $K_{d,FUR}$ = 5.1) and varying the water-to-organic solvent ratios yielded two distinct observations, as shown in Figure 9. The conversion rates of both CPO and FUR decreased significantly upon increasing the organic/water solvent ratio (Figure S4). Meanwhile, the product distribution shifted notably toward the intermediate dimeric products, rather than trimeric ones, caused by the decrease in conversion, in line with reaction kinetics (Figures

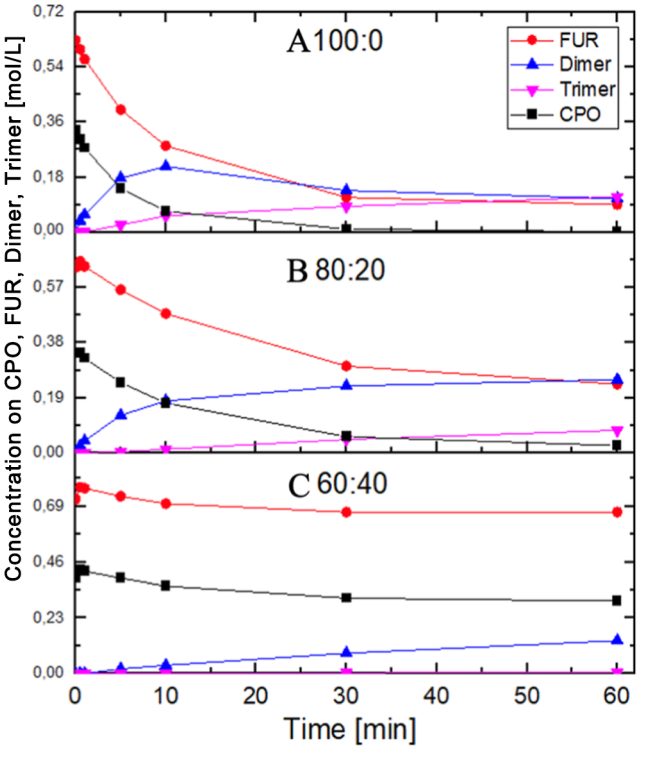

Figure 9. Comparison of kinetic profiles at different solvents ratios of water and 2-MTHF. (A) 100:0, (B) 80:20, and (C) 60:40. CPO and FUR: 2.63 and 6.0 wt % (1:2 molar), pH 12.0, 30 °C.

https://doi.org/10.1021/acssuschemeng.4c09269
ACS Sustainable Chem. Eng. XXXX, XXX, XXX−XXX

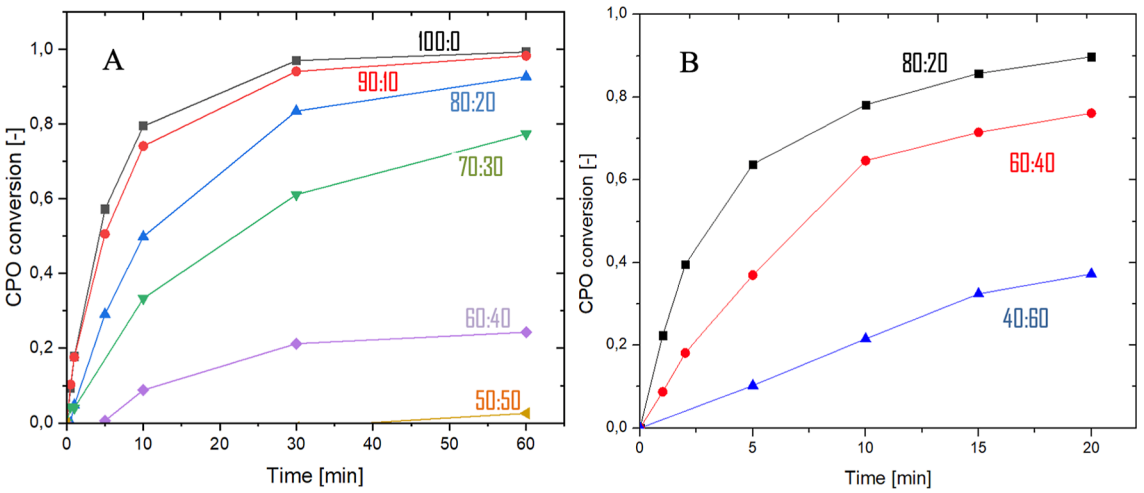

Figure 10. CPO conversion at various solvent ratios in (A) 2-MTHF and (B) octane. pH = 12.0, CPO and FUR: 2.63 and 6.0 wt % (1:2 molar), 30 °C.

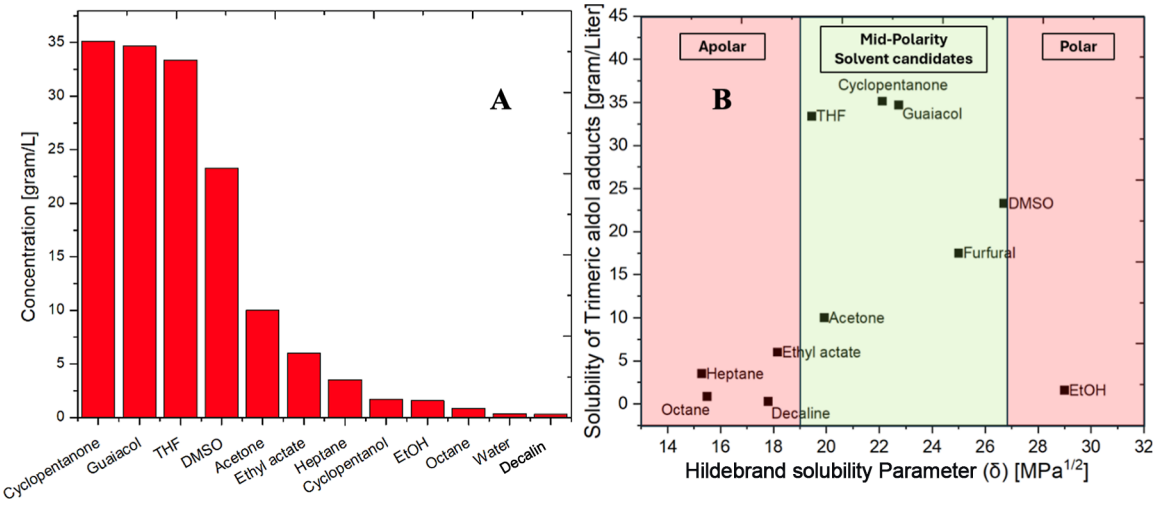

Figure 11. (A) Solubility of aldol adducts in common laboratory solvents, performed at room temperature. (B) Aldol adduct solubility compared to the Hildebrand solubility parameter.

S5 and S6). Employing other solvents having a similar K_d for reactants appear to be in agreement with the results obtained using 2-MTHF as guaiacol ($K_{d,CPO}$ = 1.2, $K_{d,FUR}$ = 4.4) also appeared to almost lose all conversion at a 1:1 solvent ratio (Figures S7 and S8). Conversely, when employing octane ($K_{d,CPO}$ = 0.6, $K_{d,FUR}$ = 0.4) or decalin ($K_{d,CPO}$ = 0.9, $K_{d,FUR}$ = 0.6), ≥90% CPO conversion could still be obtained under 1:1 solvent condition after 15−20 min of reaction (Figures 10 and S9).

The change in conversion and selectivity can be explained by the substantial differences in K_d values using the rate equations defined previously. The total reactant concentrations are distributed between the nonreactive organic phase and the reactive aqueous phase, lowering the effective concentration and subsequently its reaction rate.

Despite the positive impact of low K_d solvents on reaction performance, a significant issue remains: the persistent precipitation of reaction products during and after the reactions, which contributes to fouling of the reactor and equipment. This challenge stems from the very low solubility of the products in the most commonly used laboratory solvents. As illustrated in Figure 11A, product solubility ranges from ∼0.03% to ∼35 g/L, while the total organic feed intake consists of ∼80 g/L.

Although (apolar) alkanes demonstrate a higher rate of conversion, they do not effectively address the primary issue of product solubility, as can be observed by the Hildebrand solubility parameter (Figure 11B). For polar solvents like water (δ = 48, not shown in Figure 11B), solubility shows a marked decline. In contrast, midpolar solvents are more advantageous due to their higher product solubility when selecting the appropriate solvent, but conversion appears to drop at higher organic ratios.

This presents the direct dilemma, as illustrated in Figure 12: extracting or solubilizing the reaction products inadvertently also extracts the reactants, leading to only marginal conversion at lower water loadings. As illustrated in Figure 12, finding solvents with a high affinity for product solubilization while maintaining a low affinity for the reactants is challenging, if not impossible, due to the chemical similarity between the reactants and products.

3.7. Temperature-Controlled Solubility and Separation. To still facilitate the desired reactive extraction, the reaction could be performed at elevated temperatures to boost

https://doi.org/10.1021/acssuschemeng.4c09269
ACS Sustainable Chem. Eng. XXXX, XXX, XXX−XXX

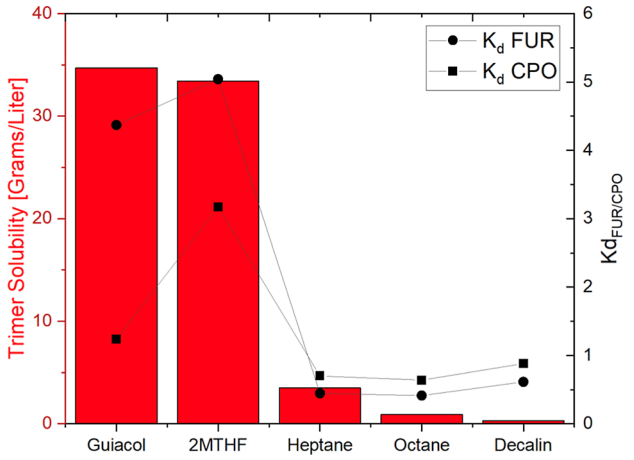

Figure 12. Aldol adduct solubility in various solvents, along with the partition coefficients of the reactants CPO and FUR.

product solubility and reaction performance. Previous work performed by Prapasawat et al. demonstrated a significant increase in product solubility in THF (~7×) and THF/water (~10×) mixtures at elevated temperatures (~35−130 °C), whereas the solubility in the pure H_2O was not significantly affected.[38] This increase in solubility at higher temperatures could enhance the efficiency of the reactive extraction process while also increasing kinetics, as determined in Figure 6. However, it would also increase the reactant solubility in the organic phase. In addition to the direct impact of process-foreign solvents on reaction performance, a major drawback is the unavoidable need for their downstream separation, which is often complex and expensive. This makes the use of such solvents undesirable.

A potential solution lies in the utilization of the process-owned solvents, as discussed in Figure 1. In this system, H_2O, FUR, hydrogenated aldol adducts (saturated oxygenates, Figure 1-VI), and the final C_{15} hydrocarbon (Figure 1-VIII) are present. Notably, saturated oxygenates and FUR exhibit a significantly higher affinity for aldol adduct solubility compared to the conventional laboratory solvents shown in Figure 11, as demonstrated in Figure 13.

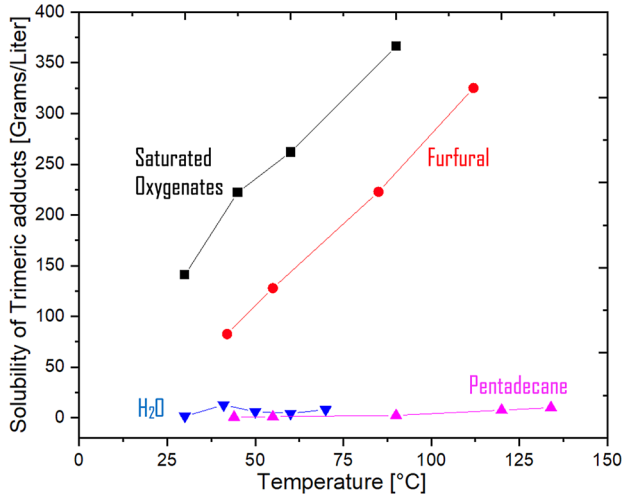

Figure 13. Experimentally determined trimeric adduct solubility in process owned solvents at various temperatures.

While this strategy helps to address product precipitation challenges, it does not fully resolve the issue of reactant extraction as FUR ($K_{d,CPO}$ = 5.2, $K_{d,FUR}$ = water saturated with FUR) and saturated oxygenates ($K_{d,CPO}$ = 2.84, $K_{d,FUR}$ = 8.9) exhibit a high extraction potential for reactants, which will negatively impact the reaction efficiency.

However, this issue may be alleviated by employing lower organic loadings (e.g., 10−20 vol %) while operating at elevated temperatures as the high solubility of aldol adducts in FUR and saturated oxygenates allows for sufficient solubilization with reduced organic content. These lower ratios, although still possessing high extraction affinity, will limit the extent of reactant extraction, thus only moderately affecting the reaction performance. This approach balances solubilization with a minimal impact on reaction efficiency. Additionally, incorporating these process-owned solvents into an integrated system could further mitigate the challenges associated with downstream solvent separation.

To test this hypothesis, a reaction with excess FUR (25 vol %) was performed at slightly lower concentrations (~3 wt % instead of ~8 wt %), corresponding to the expected maximum solubility of the trimer at this FUR volume fraction at 60 °C, (Figure 14). By carefully adjusting the reaction parameters,

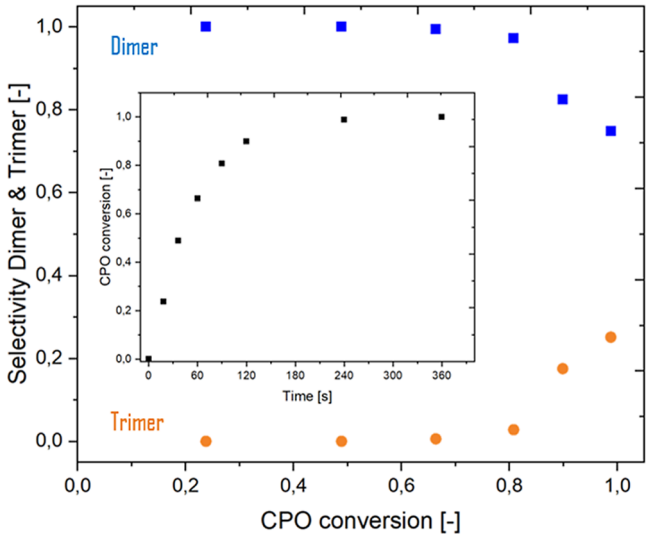

Figure 14. Aldol condensation of FUR and CPO using biphasic conditions utilizing excess FUR. 60 °C, 25 vol % FUR, 0.9 g CPO per 100 mL, 2 g FUR per 100 mL, pH = 12.75.

such as temperature and [OH^-], the reaction proceeded rapidly despite the high $K_{d,CPO}$ of FUR. Complete CPO conversion was observed within approximately 200 s. Importantly, no product precipitation was observed at these temperatures. However, when the reactor was cooled at the end of the experiment, precipitation started to occur. In addition, the reaction did not stall at the dimeric product stage, even though these intermediates could potentially dissolve and be prematurely extracted by FUR. Instead, trimeric selectivity exceeded 60% after 1200 s (Figure S9), clearly indicating the activity of the sequential coupling.

Additional separation opportunities arise from the strong temperature-dependent solubility of the aldol adducts in these process-owned solvents. Reactions were conducted at elevated temperatures to keep all components in solution and subsequently the mixture was cooled to selectively precipitate

https://doi.org/10.1021/acssuschemeng.4c09269
ACS Sustainable Chem. Eng. XXXX, XXX, XXX−XXX

the solid in dedicated equipment—thereby avoiding unwanted reactor fouling—while still utilizing solid separation. This approach also opens up possibilities for selecting solvents that are biphasic at room temperature for efficient product extraction via phase separation but become monophasic at elevated temperatures to enhance the reaction kinetics. However, identifying such solvents is expected to be challenging.

To assess the viability and desired parameters of the process-owned and other potential solvents for this application, an extended first-order kinetic model was developed to describe the biphasic system. This model builds on the initial first-order kinetic framework and incorporates observations from experimental data.

3.8. Modeling. As the reactive phase concentration is dependent on the partition coefficient and the volume of the respected phases, two adjustments need to be made to the kinetic model described above. First, the total reactant concentrations are distributed between the nonreactive organic phase and the reactive aqueous phase according to

$$V_{tot}[CPO]_{tot} = V_{aq}[CPO]_{aq} + V_{org}[CPO]_{org} \quad \text{(IX)}$$

$$K_{dCPO} = \frac{[CPO]^{org}}{[CPO]^{aq}} \qquad \text{where } [CPO]_{aq} = \frac{[CPO]^{org}}{K_{dCPO}} \quad \text{(X)}$$

In addition, there will be the need for a mass transfer term (flux term) as the reactants stored in the organic phase will need to be transported toward the aqueous reactive phase as they will be dormant otherwise, as further shown in Supporting Information, resulting in relations XI and XII. For further modeling, high kla (kla = 1000) values were used to investigate the influence parameters in the absence of mass transfer.

$$\text{Mass transfer term (org to } H_2O) = J_{CPO} = -\text{kla} \times \frac{(V_{aq} + V_{org})}{V_{aq}} \times \left(\frac{[CPO]^{org}}{K_{dCPO}} - [CPO]^{aq} \right) \quad \text{(XI)}$$

$$\frac{d[CPO]^{aq}}{dt} = -k_1[CPO]^{aq}[FUR]^{aq} + \text{kla} \times \frac{(V_{aq} + V_{org})}{V_{aq}} \times \left(\frac{[CPO]^{org}}{K_{dCPO}} - [CPO]^{aq} \right) \quad \text{(XII)}$$

3.9. Influence of the Partition Coefficient (K_d). Given that the partition coefficient emerged as a critical parameter, we utilized the model to investigate their influence on conversion at a fixed time of 60 min as a function of both $K_{d,CPO}$ and $K_{d,FUR}$ at fixed $K_{d,dimer}$ (Figure 15).

The decision to use a fixed dimer K_d of 1 may be unrealistic, given the significantly higher solubility of the dimer in most organic solvents compared to H_2O. However, it was fixed primarily to investigate the specific effect of K_d on CPO conversion. Highest CPO conversion occurs when the K_d values for both reactants are as close to 0 as possible, indicating that most reactants are in the active aqueous phase. Conversely, reactions with extremely high K_d values result in low levels of conversion as most reactants remain dormant in the organic phase and are further expected to be transport limited.

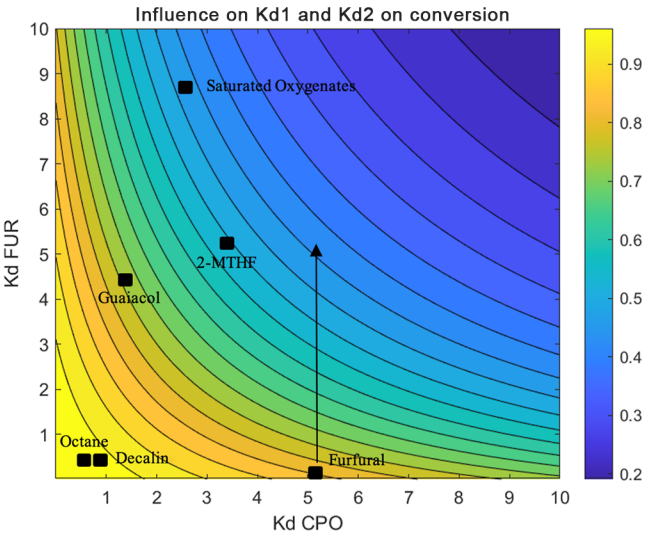

Figure 15. Modeled CPO conversion at infinitely fast mass transport (kla = 1000) as a function of both reactant partition coefficients, K_d dimer = 1, K_d trimer = 1.

Some experimentally determined K_d values of different solvents were added to Figure 15 to give more insight into solvent choice. The data point of FUR K_d-FUR might be misleading as it was difficult to determine due to the saturation of the aqueous phase being the reactant and is expected to be much higher, indicated with the black arrow. Additionally, the data indicate no significant effect of solvents on selectivity at comparable conversion but rather, there is a purely solvent effect, reactant, that slows down the reaction rates, redistributes molar ratios, and therefore influences conversion and product selectivity.

Besides a clear influence on conversion, the combination of reactants K_d values will also significantly influence the product distribution, selectivity. To investigate, the trimeric selectivity was determined as a function of both reactant K_d values at a fixed CPO conversion of 80 mol % and fixed K_d values for the products (Figure 16).

As illustrated in Figure 16, the partition coefficient of FUR (y-axis) is the most critical factor for achieving a high trimeric selectivity. Throughout the entire CPO K_d range, high selectivity toward trimer formation was consistently observed, driven by the shift toward a higher stoichiometric ratio of FUR compared to CPO. In contrast, solvents with a higher affinity for FUR notably reduce the selectivity for the desired trimeric product, necessitating longer reaction times to achieve full conversion toward the trimeric products. The data clearly show that the choice of organic solvent significantly influences product distribution, enabling fine-tuning of selectivity by simply changing the solvent while varying reaction time and conversion, besides the obvious change of CPO to FUR ratios. For instance, solvents such as octane, decalin, and FUR result in high trimeric selectivity, while solvents like guaiacol, saturated oxygenates, and 2-MTHF tend to favor dimeric adducts or would require significantly longer residence times to drive the reaction toward trimeric adduct formation.

In addition to the partition coefficients of the reactants, the partition coefficients of the products are equally important. Due to the chemical similarity in polarity between reactants

https://doi.org/10.1021/acssuschemeng.4c09269
ACS Sustainable Chem. Eng. XXXX, XXX, XXX−XXX

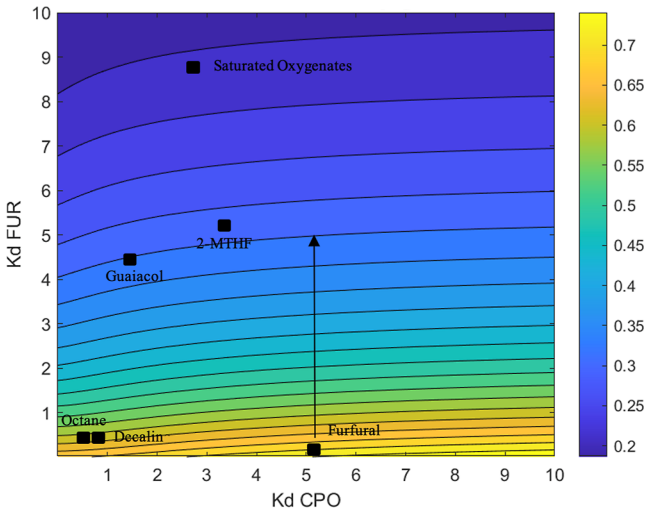

Figure 16. Selectivity of trimer as a function of reactant partition coefficients at fixed CPO conversion of 80 mol % at infinitely fast mass transport (kla = 1000). K_d dimer = 1, K_d trimer = 1.

and products, there is a significant risk of prematurely extracting products, causing the reaction to halt at the C10 stage. The trimeric selectivity at a fixed CPO conversion of 90 mol % illustrates product selectivity as a function the partition coefficient of the dimer ($K_{d,dimer}$) conversion (Figure 17A). When using excessively strong extraction solvents or working at concentrations higher than the maximum solubility of adducts in water, achieving the desired C15 adducts requires significantly increased residence times to ensure the conversion of dimeric species into the desired trimeric products. Figure 17B illustrates the trimeric selectivity in the case where K_d for the reactants equals K_d for the products. By varying solvents and carefully selecting the K_d values for the dimer and reactants, it is possible to produce dimeric adducts over trimeric ones by simply adjusting these K_d/solvent.

3.10. Process Concept. Running the aldol condensation of FUR and CPO in a biphasic system offers key advantages, including the elimination of challenges such as equipment fouling. Additionally, this approach provides opportunities for better control over product selectivity through the strategic selection of solvents, besides aqueous running at a lower FUR/CPO ratio.

As outlined in Figure 18, the reactor effluent from R1 can be efficiently separated using a phase separator, S-1, which enables recycling of the caustic aqueous stream back into the aldol reactor. Three potential solvents are of particular interest, namely, FUR, the saturated oxygenates from reactor R2, and the final hydrocarbon biojet from reactor R3. These solvents are particularly attractive due to their availability as process-owned solvents.

Of the three options, FUR and saturated oxygenates stand out due to their high aldol solubility (Figure 13), which effectively prevents fouling. Their key differences lie in their partition coefficients for the reactants, as shown in Figures 15 and 16 in terms of conversion and selectivity. While both solvents exhibit relatively high partition coefficients for the reactants, FUR emerges as the more favorable choice due to its ability to saturate the aqueous phase with FUR-reactant as this is observed to be the key parameter in high trimeric selectivity (Figure 16). Although FUR has a higher $K_{d,CPO}$ than the saturated oxygenates, this higher partition coefficient can enhance product selectivity and still achieve relatively high conversion rates, making FUR the preferred solvent.

However, a key challenge with using FUR is its susceptibility to extensive hydrotreatment in reactors R2 and R3, which leads to the formation of undesirable byproducts, necessitating its separation before these stages. To address this issue, distillation (S-2) is proposed for separating FUR, unreacted CPO, and H_2O from the reaction mixture. To prevent solid precipitation during distillation, a cosolvent is required, with the saturated oxygenates being ideally suited for this purpose due to their high aldol solubility and the opportunity for process integration.

By utilizing both FUR and the saturated oxygenates—either as biphasic solvents in R1 or as cofeeds to enhance aldol adduct solubility prior to distillation—an integrated process can be developed.

This system allows for the efficient recycling of both the aqueous phase and the organic solvents. The organic solvents can be regenerated via distillation and returned to the aldol reactor, while the aldol products, dissolved in the saturated

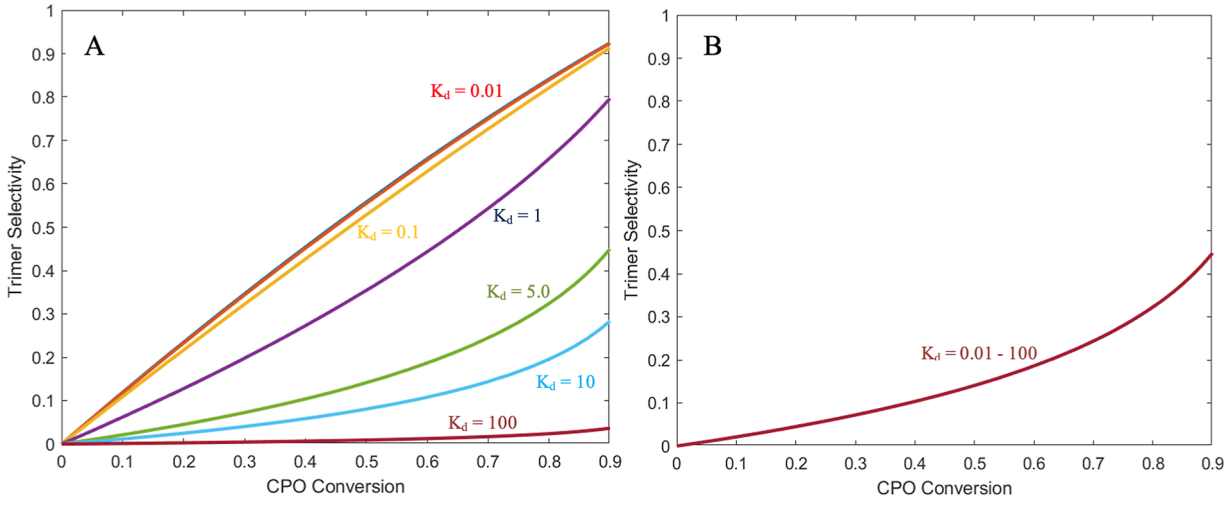

Figure 17. (A) Influence of K_d dimer on the trimeric selectivity at 90 mol % conversion of CPO using kla = 1000, $k_{d,CPO}$ = 1 and $k_{d,FUR}$ = 1, solvent ratio 1:1. (B) $K_{d,reactant}$ equals $K_{d,dimer}$.

https://doi.org/10.1021/acssuschemeng.4c09269
ACS Sustainable Chem. Eng. XXXX, XXX, XXX−XXX

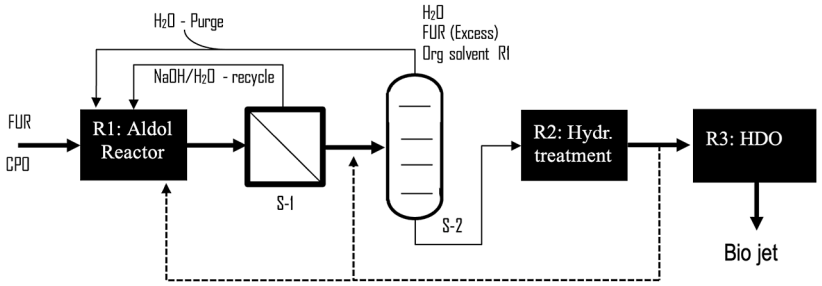

Figure 18. Conceptual process design for the integration of homogeneous catalyzed aldol coupling making use of reactive extraction.

oxygenates or final jet fuel, can be hydrotreated to produce the final jet fuel.

While the biphasic approach offers significant potential for enhancing product solubility and avoiding solid handling, it also presents several challenges. Running reactions with excess FUR requires a larger reactor (R2) to maintain reactor productivity, increases distillation demands in S-2, and introduces complexities related to premature reactant and product extraction, leading to a lighter product slate. To overcome this, reactions would need to be run for considerably longer durations to shift the selectivity toward trimeric C15. Despite these drawbacks, the biphasic approach still provides key advantages over the monophasic system proposed in the literature. Unlike monophasic systems, it avoids the need to distill all the solvent (water and cosolvent) to recover the product as most caustic water can be easily recycled through phase separation. However, detailed process modeling and economic analysis are required to quantify the cost−benefit ratio of biphasic operation.

4. CONCLUSIONS

The condensation of CPO and FUR in aqueous caustic medium is well described by a simple kinetic model that is first order in CPO, FUR, and dimeric intermediate. The results underscore the necessity of operating under highly alkaline conditions with significant conversion achieved at pH 12 and higher. The activation energies for the formation of the dimer and trimer were found to be similar at approximately 75 kJ/mol.

The precipitation of the desired trimeric product could be alleviated by adding a polar but water-insoluble organic solvent and running the reaction under biphasic conditions at an elevated temperature. An extended first-order kinetic model gave insight into the importance of partition coefficients of reactants and product on both reaction conversion and selectivity. It thereby highlights the challenge of finding a solvent that is effective in extracting the trimeric product while leaving most of the reactant and the dimeric intermediate in the aqueous phase.

Based on these insights, a process concept was proposed that circumvents reactor and equipment fouling by employing process-owned solvents.

ASSOCIATED CONTENT

Supporting Information

The Supporting Information is available free of charge at https://pubs.acs.org/doi/10.1021/acssuschemeng.4c09269.

Additional experimental data, parity plots, sensitivity analyses, and other supplementary figures (PDF)

AUTHOR INFORMATION

Corresponding Author

M. Pilar Ruiz − *Sustainable Process Technology, Faculty of Science and Technology, University of Twente, 7522 NB Enschede, The Netherlands;* orcid.org/0000-0003-1437-5578; Email: m.p.ruizramiro@utwente.nl

Authors

Rick Baldenhofer − *Sustainable Process Technology, Faculty of Science and Technology, University of Twente, 7522 NB Enschede, The Netherlands*

Jean-Paul Lange − *Sustainable Process Technology, Faculty of Science and Technology, University of Twente, 7522 NB Enschede, The Netherlands*

Sascha R. A. Kersten − *Sustainable Process Technology, Faculty of Science and Technology, University of Twente, 7522 NB Enschede, The Netherlands;* orcid.org/0000-0001-8333-2649

Complete contact information is available at: https://pubs.acs.org/10.1021/acssuschemeng.4c09269

Notes

The authors declare no competing financial interest.

ACKNOWLEDGMENTS

The authors would like to thank Shell Global Solutions International B.V., Auke Smet, Fiona Hafferl, Benno Knaken, Ronald Borst, Johan Agterhorst, Raymond Spanjer, and Erna Fränzel-Luiten for their invaluable technical support and expertise.

REFERENCES

(1) Dolšak, N.; Prakash, A. Different Approaches to Reducing Aviation Emissions: Reviewing the Structure-Agency Debate in Climate Policy. *Clim. Action* **2022**, *1* (1), 2.

(2) Watson, M. J.; Machado, P. G.; da Silva, A. V.; Saltar, Y.; Ribeiro, C. O.; Nascimento, C. A. O.; Dowling, A. W. Sustainable Aviation Fuel Technologies, Costs, Emissions, Policies, and Markets: A Critical Review. *J. Cleaner Prod.* **2024**, *449*, 141472.

(3) Cabrera, E.; de Sousa, J. M. M. Use of Sustainable Fuels in Aviation—A Review. *Energies* **2022**, *15*, 2440.

(4) Ng, K. S.; Farooq, D.; Yang, A. Global Biorenewable Development Strategies for Sustainable Aviation Fuel Production. *Renewable Sustainable Energy Rev.* **2021**, *150*, 111502.

(5) Timmons, D.; Terwel, R. Economics of Aviation Fuel Decarbonization: A Preliminary Assessment. *J. Cleaner Prod.* **2022**, *369*, 133097.

(6) Makhova, U. A.; Ershov, M. A.; Ilin, A. V.; Savelenko, V. D.; Burov, N. O.; Lobashova, M. M.; Sharin, E. A.; Shevtsov, A. A.; Vikhritskaya, A. O.; Kapustin, V. M.; Abdellatief, T. M. M. Green Approach to Alternative Fuel for Jet Fuel Quality Issues in the

Perspective of Decarbonization. *Process Saf. Environ. Prot.* **2024**, *188*, 905−916.
(7) Song, M.; Zhang, X.; Chen, Y.; Zhang, Q.; Chen, L.; Liu, J.; Ma, L. Hydroprocessing of Lipids: An Effective Production Process for Sustainable Aviation Fuel; Energy, 2023; Vol. *283*, p 129107..
(8) Główka, M.; Wójcik, J.; Boberski, P.; Białecki, T.; Gawron, B.; Skolniak, M.; Suchocki, T. Sustainable Aviation Fuel − Comprehensive Study on Highly Selective Isomerization Route towards HEFA Based Bioadditives. *Renewable Energy* **2024**, *220*, 119696.
(9) Eyberg, V.; Dieterich, V.; Bastek, S.; Dossow, M.; Spliethoff, H.; Fendt, S. Techno-Economic Assessment and Comparison of Fischer−Tropsch and Methanol-to-Jet Processes to Produce Sustainable Aviation Fuel via Power-to-Liquid. *Energy Convers. Manage.* **2024**, *315*, 118728.
(10) Ruokonen, J.; Nieminen, H.; Dahiru, A. R.; Laari, A.; Koiranen, T.; Laaksonen, P.; Vuokila, A.; Huuhtanen, M. Modelling and Cost Estimation for Conversion of Green Methanol to Renewable Liquid Transport Fuels via Olefin Oligomerisation. *Processes* **2021**, *9* (6), 1046.
(11) Aguayo, A. T.; Mier, D.; Gayubo, A. G.; Gamero, M.; Bilbao, J. Kinetics of Methanol Transformation into Hydrocarbons on a HZSM-5 Zeolite Catalyst at High Temperature (400−550°c). *Ind. Eng. Chem. Res.* **2010**, *49* (24), 12371−12378.
(12) Shehab, M. *Production of Sustainable Aviation Fuel through Biomass: Experimental and Simulation Approach*; University of Twente: Enschede, The Netherlands, 2024.
(13) Geleynse, S.; Brandt, K.; Garcia-Perez, M.; Wolcott, M.; Zhang, X. The Alcohol-to-Jet Conversion Pathway for Drop-In Biofuels: Techno-Economic Evaluation. *ChemSusChem* **2018**, *11* (21), 3728−3741.
(14) Liu, Z.; Liao, J.; Gong, Y.; Song, J.; Wang, T. Efficient Production of Jet-Fuel Precursors via One-Pot Dehydration-Oligomerization of Higher Alcohols from Upgrading of Bioethanol. *Energy Convers. Manage.* **2024**, *299*, 117833.
(15) Zhong, Q.; Liao, J.; Zhang, Q.; Qiu, S.; Meng, Q.; Wu, X.; Wang, T. Aqueous Upgrading of Ethanol to Higher Alcohol Diesel Blending and Jet Fuel Precursors over Na-Doped Porous Ni@C Nanocomposite. *Fuel* **2022**, *324*, 124507.
(16) Kunamalla, A.; Maity, S. K. Production of Green Jet Fuel from Furanics via Hydroxyalkylation-Alkylation over Mesoporous MoO3-ZrO2 and Hydrodeoxygenation over Co/γ-Al2O3: Role of Calcination Temperature and MoO3 Content in MoO3-ZrO2. *Fuel* **2023**, *332*, 125977.
(17) Yan, P.; Wang, H.; Liao, Y.; Wang, C. Synthesis of Renewable Diesel and Jet Fuels from Bio-Based Furanics via Hydroxyalkylation/Alkylation (HAA) over SO42-/TiO2 and Hydrodeoxygenation (HDO) Reactions. *Fuel* **2023**, *342*, 127685.
(18) Gathergood, N.; Granados, M.; Martin Alonso, D. *Furfural − an Entry Point of Lignocellulose in Biorefineries to Produce Renewable Chemicals, Polymers and Biofuels*; World Scientific, 2018.
(19) Cueto, J.; Rapado, P.; Faba, L.; Díaz, E.; Ordóñez, S. From Biomass to Diesel Additives: Hydrogenation of Cyclopentanone-Furfural Aldol Condensation Adducts. *J. Environ. Chem. Eng.* **2021**, *9* (4), 105328.
(20) Barrett, C. J.; Chheda, J. N.; Huber, G. W.; Dumesic, J. A. Single-Reactor Process for Sequential Aldol-Condensation and Hydrogenation of Biomass-Derived Compounds in Water. *Appl. Catal., B* **2006**, *66* (1−2), 111−118.
(21) Ao, L.; Zhao, W.; Guan, Y.; Wang, D.; Liu, K.; Guo, T.; Fan, X.; Wei, X. Efficient Synthesis of C15 Fuel Precursor by Heterogeneously Catalyzed Aldol-Condensation of Furfural with Cyclopentanone. *RSC Adv.* **2019**, *9* (7), 3661−3668.
(22) Lange, J.; van der Heide, E.; van Buijtenen, J.; Price, R. Furfural—A Promising Platform for Lignocellulosic Biofuels. *ChemSusChem* **2012**, *5*, 150−166.
(23) Ricciardi, L.; Verboom, W.; Lange, J. P.; Huskens, J. Production of Furans from C5and C6sugars in the Presence of Polar Organic Solvents. *Sustainable Energy Fuels* **2022**, *6*, 11−28.
(24) Jaswal, A.; Singh, P. P.; Mondal, T. Furfural-a Versatile, Biomass-Derived Platform Chemical for the Production of Renewable Chemicals. *Green Chem.* **2022**, *24*, 510−551.
(25) Lange, J. P. Furfural Manufacture and Valorization − A Selection of Recent Developments. *Catal. Today* **2024**, *435*, 114726.
(26) van der Wal, P. J.; Lange, J. P.; Kersten, S. R. A.; Ruiz, M. P. Kinetics of Furfural Formation from Xylose via a Boronic Ester Intermediate. *ACS Sustain. Chem. Eng.* **2024**, *12* (6), 2412−2420.
(27) Van Der Wal, P. J.; Kersten, S. R. A.; Lange, J. P.; Ruiz, M. P. Process Development on the High-Yielding Reactive Extraction of Xylose with Boronic Acids. *Ind. Eng. Chem. Res.* **2023**, *62* (20), 8002−8009.
(28) Ricciardi, L.; Verboom, W.; Lange, J. P.; Huskens, J. Kinetic Model for the Dehydration of Xylose to Furfural from a Boronate Diester Precursor. *RSC Adv.* **2022**, *12* (49), 31818−31829.
(29) Lange, J. P. Renewable Feedstocks: The Problem of Catalyst Deactivation and Its Mitigation. *Angew. Chem., Int. Ed.* **2015**, *54* (45), 13186−13197.
(30) Baldenhofer, R.; Lange, J.-P.; Kersten, S. R. A.; Ruiz, M. P. Furfural to Cyclopentanone − a Search for Putative Oligomeric by-Products. *ChemSusChem* **2024**, *17* (12), No. e202400108.
(31) Piutti, C.; Quartieri, F. The Piancatelli Rearrangement: New Applications for an Intriguing Reaction. *Molecules* **2013**, *18* (10), 12290−12312.
(32) Piancatelli, G.; Scettri, A.; Barbadoro, S. A Useful Preparation of 4-Substituted 5-Hydroxy-3-Oxocyclopentene. *Tetrahedron Lett.* **1976**, *17* (39), 3555−3558.
(33) Patil, A.; Engelbert van Bevervoorde, M. J. S.; Neira D'Angelo, F. Intensifying Cyclopentanone Synthesis from Furfural Using Supported Copper Catalysts. *ChemSusChem* **2024**, No. e202401484.
(34) Muldoon, J. A.; Harvey, B. G. Bio-Based Cycloalkanes: The Missing Link to High-Performance Sustainable Jet Fuels. *ChemSusChem* **2020**, *13*, 5777−5807.
(35) Baldenhofer, R.; Smet, A.; Lange, J. P.; Kersten, S. R. A.; Ruiz, M. P. Furanic Jet Fuels − Water-Free Aldol Condensation of Furfural and Cyclopentanone. *Biomass Bioenergy* **2024**, *190*, 107410.
(36) Cueto, J.; Faba, L.; Díaz, E.; Ordóñez, S. Enhancement of Furfural−Cyclopentanone Aldol Condensation Using Binary Water−Ethanol Mixtures as Solvent. *J. Chem. Technol. Biotechnol.* **2018**, *93* (6), 1563−1571.
(37) De Saint Laumer, J. Y.; Cicchetti, E.; Merle, P.; Egger, J.; Chaintreau, A. Quantification in Gas Chromatography: Prediction of Flame Ionization Detector Response Factors from Combustion Enthalpies and Molecular Structures. *Anal. Chem.* **2010**, *82*, 6457−6462.
(38) Prapasawat, T.; Hronec, M.; Štolcová, M.; Lothongkum, A. W.; Pancharoen, U.; Phatanasri, S. Thermodynamic Models for Determination of the Solubility of 2,5-Bis(2-Furylmethylidene)-Cyclopentan-1-One in Different Solvents at Temperatures Ranging from 308.15 to 403.15K. *Fluid Phase Equilib.* **2014**, *367*, 57−62.

https://doi.org/10.1021/acssuschemeng.4c09269
ACS Sustainable Chem. Eng. XXXX, XXX, XXX−XXX